



Alginate-based hydrogels with improved adhesive properties for cell encapsulation



Bapi Sarker^a, Julia Rompf^{a,b}, Raquel Silva^a, Nadine Lang^b, Rainer Detsch^a, Joachim Kaschta^c, Ben Fabry^b, Aldo R. Boccaccini^{a,*}

^a Institute of Biomaterials, Department of Materials Science and Engineering, University of Erlangen-Nuremberg, 91058 Erlangen, Germany

^b Department of Physics, University of Erlangen-Nuremberg, 91052 Erlangen, Germany

^c Institute of Polymer Materials, Department of Materials Science and Engineering, University of Erlangen-Nuremberg, 91058 Erlangen, Germany

ARTICLE INFO

Article history:

Received 20 January 2015

Received in revised form 26 March 2015

Accepted 29 March 2015

Available online 4 April 2015

Keywords:

Cell encapsulation

Hydrogel

Alginate

ABSTRACT

Hydrogel-based biomaterials are ideal scaffolding matrices for microencapsulation, but they need to be modified to resemble the mechanical, structural and chemical properties of the native extracellular matrix. Here, we compare the mechanical properties and the degradation behavior of unmodified and modified alginate hydrogels in which cell adhesive functionality is conferred either by blending or covalently cross-linking with gelatin. Furthermore, we measure the spreading and proliferation of encapsulated osteoblast-like MG-63 cells. Alginate hydrogels covalently crosslinked with gelatin show the highest degree of cell adhesion, spreading, migration, and proliferation, as well as a faster degradation rate, and are therefore a particularly suitable material for microencapsulation.

© 2015 Elsevier B.V. All rights reserved.

1. Introduction

Cell encapsulation – the immobilization of cells in polymeric hydrogels – is a promising technique in tissue engineering [1]. Hydrogels can act as a semipermeable membrane, which protect the encapsulated cells from the host's immune system while allowing for the bidirectional diffusion of oxygen, nutrients and waste. Moreover, hydrogels attenuate the mechanical stress and friction not only on encapsulated cells but also on adjacent tissue upon transplantation [1–4]. The material of choice for many cell encapsulation applications is alginate because of its biocompatibility and rapid ionic gelation property with divalent cation [5,6]. Alginate represents a family of anionic polysaccharides extracted from brown algae or bacteria. They are linear unbranched copolymers composed of (1–4)-linked β -D-mannuronic acid (M) and α -L-guluronic acid (G) monomers [7–9]. The fraction and sequence of M- and G-monomers vary with the origin of alginate and contribute to different chemical and physical properties [10]. When the G-blocks of neighboring polymer chains are linked with each other through divalent cation bridges, for example Ca^{2+} , alginate forms a hydrogel with viscoelastic properties [11]. However, alginate does not promote cell adhesion and proliferation due to the absence of

cell adhesion motifs. It has been shown in previous studies that cell adhesion to alginate hydrogels can be achieved by modification of alginate through functionalization with gelatin [12,13]. Gelatin is a biodegradable protein, produced by denaturation of collagen, which transforms the triple helix structure of collagen into a random coil structure [14] and thereby exposes the cell adhesion motif RGD (Arg-Gly-Asp) of collagen [15,16].

In a previous study, we established that alginate hydrogels that were functionalized by crosslinking with gelatin promoted better adhesion, proliferation, and migration of encapsulated osteoblast-like MG-63 cells compared to pure alginate hydrogels or to hydrogels functionalized with the specific integrin binding sequence RGD [12]. However, it has remained an open question whether the presence of gelatin on its own, e.g. by blending with alginate, would be sufficient for cell adhesion, migration, and proliferation, or whether gelatin must be crosslinked with alginate. Furthermore, it is unknown if the presence of gelatin speeds up the degradation behavior of the hydrogel over time and thereby promotes cell migration and proliferation. Finally, it is unknown how stably the gelatin is bound or contained in the hydrogel, or how quickly it is released over time into the surrounding medium.

In this study we compared the behavior of osteoblast-like MG-63 cells in two alginate hydrogel systems that were functionalized with gelatin either by covalent crosslinking of alginate di-aldehyde and gelatin (ADA-GEL-x), or by simple blending of alginate and gelatin prior to polymerization (ALG-GEL-b). We embedded the

* Corresponding author. Tel.: +49 9131 85 28601; fax: +49 9131 85 28602.
E-mail address: aldo.boccaccini@ww.uni-erlangen.de (A.R. Boccaccini).

cells in hydrogel capsules of 800 μm diameter, and characterized cell viability, mitochondrial activity, spreading morphology and hydrogel degradation over a time course of up to 28 days. ADA-GEL-x hydrogels facilitated superior adhesion, proliferation, migration, and morphology of encapsulated cells compared to ALG-GEL-b. Moreover, the gelatin release kinetics was slower in ADA-GEL-x compared to ALG-GEL-b, yet the overall hydrogel degradation rate as evaluated from the decrease in stiffness of microcapsules over time was higher. Thus, we conclude that the better adhesion, proliferation, and migration of encapsulated osteoblast-like MG-63 cells in gelatin-crosslinked alginate hydrogel microcapsules arises as a combination of a stronger binding of gelatin to the hydrogel matrix, and a faster mechanical degradation behavior that better accommodates the proliferation and migration of embedded cells.

2. Materials and methods

2.1. Preparation of functionalized alginate gels

Sodium alginate (sodium salt of alginic acid from brown algae, suitable for immobilization of micro-organisms, guluronic acid content 65–70%) and gelatin (from porcine skin, suitable for cell culture, Type A, Bloom 300) were obtained from Sigma–Aldrich, Germany. Ethanol, ethylene glycol, sodium metaperiodate and calcium chloride dehydrate ($\text{CaCl}_2 \cdot 2\text{H}_2\text{O}$) were purchased from VWR International, Germany. Silver nitrate was obtained from Alfa Aesar, USA.

Sodium alginate was dissolved in PBS, and gelatin was dissolved in ultrapure water at 37 °C. Alginate–gelatin blend material (ALG-GEL-b) was prepared by mixing aqueous solution of gelatin with alginate solution with a volume ratio of 80:20, resulting in a final concentration of alginate and gelatin of 2% (w/v) and 0.5% (w/v), respectively.

Alginate–gelatin crosslinked hydrogel (ADA-GEL-x) was synthesized by covalent crosslinking of alginate di-aldehyde (ADA) and gelatin as described in [2]. Briefly, ADA was synthesized through controlled oxidation of sodium alginate in equal volume of an ethanol–water mixture. Sodium alginate was dispersed in ethanol and mixed with an aqueous solution of sodium metaperiodate (oxidizing agent). The suspension was stirred in dark conditions at room temperature for 6 h. The oxidation reaction was stopped by adding ethylene glycol, and the dispersion was dialyzed for 7 days against ultrapure water (Direct-Q, Merck Millipore, Germany) using a dialysis membrane (molecular weight cutoff of 6–8 kDa; Spectrum Lab, USA) to ensure complete removal of sodium metaperiodate. The absence of sodium metaperiodate in the dialysate was checked by adding 1% (w/v) solution of silver nitrate and was confirmed when no precipitation occurred. Afterwards, the ADA solution was lyophilized to obtain dry ADA, which was then dissolved in PBS to get 5% (w/v) solution. To synthesize ADA-GEL-x, 5% (w/v) aqueous solution of gelatin was mixed with 5% (w/v) solution of ADA. The final concentrations of ADA and gelatin were 2.5% (w/v). 2% (w/v) pure alginate (ALG) solution (PBS as solvent) was used as control.

2.2. Cell culture

Osteoblast-like MG-63 cells (LGC, ATCC, Germany) were used for encapsulation. DMEM culture medium (Dulbecco's modified Eagle's medium, Gibco, Germany) was supplemented with 10 vol.% fetal bovine serum (FBS, Sigma–Aldrich, Germany) and 1 vol.% penicillin–streptomycin (PS, Sigma–Aldrich, Germany). Cells were cultured at 37 °C in 95% relative humidity and 5% CO_2 , and passaged using standard protocols.

2.3. Preparation of microcapsules and cell encapsulation

Microcapsules from the three different materials were produced by a pneumatic extrusion technique as described elsewhere [2]. Briefly, the solutions of ALG, ALG-GEL-b and ADA-GEL-x were filled into a cartridge (Nordson EFD, USA) and connected to a high precision fluid dispenser (UltimusTMV, Nordson EFD, USA). Solutions were extruded by applying a controlled pressure, collected in a 0.1 M CaCl_2 solution, and kept for 10 min to facilitate ionic gelation. The prepared microcapsules were sieved and washed with ultrapure water. For cell encapsulation, the alginate and ADA solutions were sterilized by filtration through a 0.45 μm filter (Carl Roth GmbH + Co. KG, Germany), and the gelatin solution was sterilized by filtration through a 0.22 μm filter. After that, hydrogels were prepared in sterile condition. Osteoblast-like MG-63 cells were mixed with ALG, ALG-GEL-b or ADA-GEL-x at a concentration of 1×10^6 cells per 1 ml of hydrogel solution, and then extruded into microcapsules as described above. The microcapsules with embedded cells were washed with DMEM and incubated in 95% relative humidity and 5% CO_2 at 37 °C. The cell culture medium was replaced every second day.

2.4. Characterization of hydrogel properties

2.4.1. Mechanical properties

Mechanical properties of hydrogel films were measured with a dynamic-mechanical analyzer (DMTA IV, Rheometric Scientific). Measurements were performed at 25 °C in a dynamic frequency sweep (0.1–20 Hz), at which a sinusoidal deformation of constant amplitude was applied to a hydrogel film of a cylindrical shape with a diameter of 16 mm and a thickness of 1 mm. To measure the degradation kinetics of the hydrogels, the fabricated films from the three different hydrogels were incubated in DMEM at 37 °C in 95% relative humidity and 5% CO_2 , and repeatedly measured with DMTA over a time course of 28 days. All measurements were carried out in the linear viscoelastic regime at a strain of $\varepsilon = 0.1\%$. Measurements were recorded in triplicate, and the results are expressed as mean \pm one standard deviation.

2.4.2. Protein release

Weighted amounts (50 mg) of hydrogel microcapsules were immersed in 2 ml of Hank's balanced salt solution (HBSS) at 37 °C. At selected times, the supernatant was removed, collected for gelatin release analysis, and 2 ml of fresh HBSS solution was added to the samples. Protein concentration in the supernatant was determined using the Lowry method [17,18], with bovine serum albumin (BSA) as a standard [19]. The absorbance at 750 nm was measured using a UV–Vis spectrophotometer (Specord 40, Analytik Jena, Germany) [13]. The release of gelatin from the samples was calculated as follows:

$$\text{Gelatin release (\%)} = \frac{[\text{Gelatin}]_{\text{supernatant}}}{[\text{Gelatin}]_{\text{total}}} \times 100$$

where $[\text{Gelatin}]_{\text{total}}$ is the initial amount of gelatin, and $[\text{Gelatin}]_{\text{supernatant}}$ is the cumulative amount of gelatin in the supernatant at different incubation time points.

The molecular mass distribution of released protein fragments was determined by sodium dodecyl sulfate–polyacrylamide gel electrophoresis (SDS–PAGE) (Mini-PROTEAN 3 system, Bio-Rad). Polyacrylamide gels, with a concentration of 10% acrylamide and a thickness of 1 mm, were run at a constant voltage of 120 V. The Prestained Page Ruler marker (Thermo Scientific) was used for calibration. The visualization of the protein bands was performed using silver staining (Pierce Color Silver Stain Kit, Thermo Scientific).

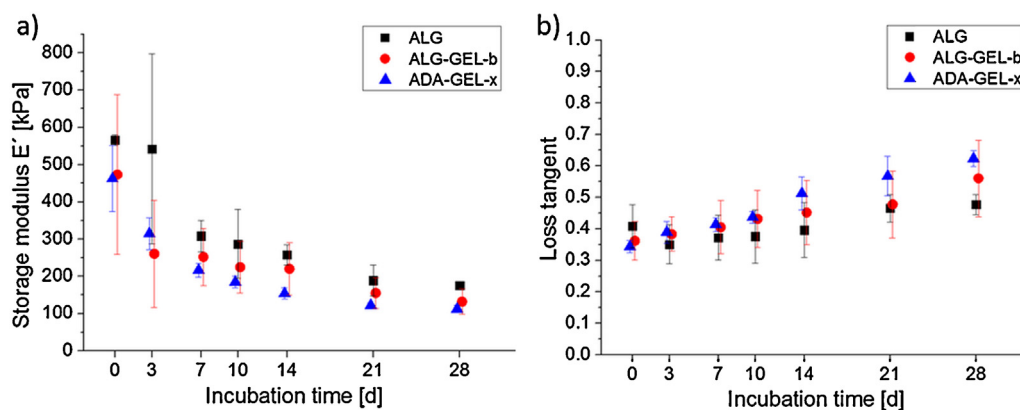


Fig. 1. (a) Storage modulus, and (b) loss tangent of ALG, ALG-GEL-b and ADA-GEL-x hydrogels measured at a frequency of 1 Hz with DMTA after immersion in DMEM at 37 °C and after different time periods of 0, 3, 7, 10, 14, 21, and 28 days (mean \pm sd of $n = 5$ measurements). To better visualize error bars, overlapping data points are slightly shifted in time.

2.4.3. Determination of microcapsules size

To investigate the change in diameter of the microcapsules over a period of 28 days, 30 microcapsules of each hydrogel type (ALG, ALG-GEL-b and ADA-GEL-x) either with or without cells were incubated in DMEM at 37 °C. The diameter of the microcapsules was measured in regular time intervals with bright-field light microscopy (Primo Vert, Carl Zeiss, Germany).

2.4.4. Cell behavior

Mitochondrial activity of the encapsulated cells was assessed through the enzymatic conversion of tetrazolium salt (WST-8 assay kit, Sigma–Aldrich, Germany) at different time points of culture. The morphology of the encapsulated cells in different hydrogels was visualized with bright-field light microscopy (Primo Vert, Carl Zeiss, Germany) after 7 and 28 days of culture. Actin cytoskeleton staining was performed with rhodamine phalloidin (Invitrogen, USA), and nuclei staining with Sytox (Invitrogen, USA). Images were taken with a confocal laser scanning microscope (SP5X, Leica, Germany) using a 20 \times dip-in water immersion objective (NA = 1.0).

2.4.5. Statistical analysis

All results are presented as arithmetic mean \pm one standard deviation. Differences in mitochondrial activity of cells were evaluated by one-way analysis of variance (ANOVA). The pairwise comparison of the means was performed with a Bonferroni's test (post hoc comparison). Differences were considered as statistically significant for p -values < 0.05.

3. Results and discussion

3.1. Material characterization

3.1.1. Mechanical analysis

Fig. 1 shows the storage modulus and loss tangent of all materials measured by DMTA immediately after their preparation and over time of up to 28 days of incubation in DMEM at 37 °C.

ALG exhibited the highest storage modulus (570 kPa at 1 Hz) immediately after preparation, as there is no additional material hindering the cross-linking of alginate G-blocks. This value is found to be higher compared to the storage modulus (~100 kPa) of ALG as reported by Hunt et al. [20]. However, it should be highlighted that the storage modulus of ALG depends on several factors, such as source of ALG, molar mass, M/G ratio, concentration of ALG solution and ionic crosslinker, etc. [21]. Indeed there was no major difference in the moduli of ALG-GEL-b and ADA-GEL-x hydrogels

(470 and 460 kPa, respectively, at 1 Hz). The moduli of ALG-GEL-b showed a larger standard deviation, however. After 28 days of incubation, the modulus of ALG decreased to 30% of its initial value compared to 28% for ALG-GEL-b and 25% for ADA-GEL-x gels. Hence, ADA-GEL-x hydrogel showed the highest degradation rate. Storage moduli and loss tangent of the three hydrogels measured at different frequencies (0.1–20 Hz) and at different incubation times are presented in the Supplementary Fig. S1. The frequency independency of the loss tangent is a rheological proof that the materials are in the gel state [22]. The increase of the loss tangent with degradation time supports the finding that the viscoelastic deformation behavior is shifted toward a less elastic behavior viz. higher energy losses due to increasing viscous deformation processes.

Supplementary material related to this article can be found, in the online version, at <http://dx.doi.org/10.1016/j.ijbiomac.2015.03.061>.

Degradation and softening of the hydrogels over time is caused by diffusive release of calcium ions that form the cross-links between alginate G-blocks [23,24]. Our results of a more stable behavior of unmodified alginate compared to ADA-GEL-x and ALG-GEL-b is consistent with a lower diffusion of ions due to the higher crosslinking density. Moreover, diffusion of gelatin from the

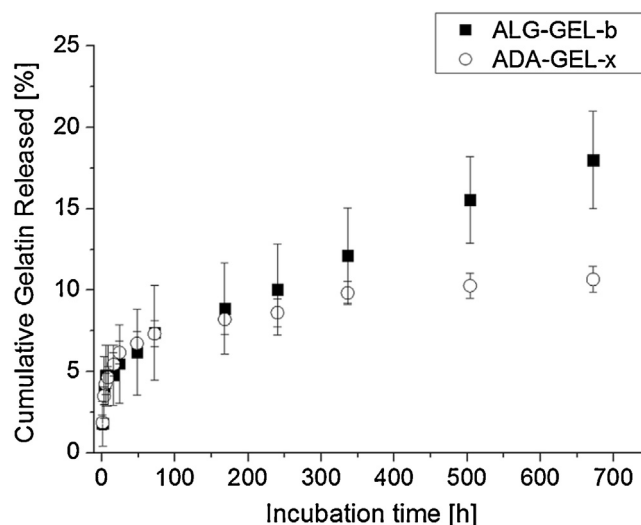


Fig. 2. Cumulative gelatin released from ALG-GEL-b and ADA-GEL-x hydrogels over a period of 28 days in HBSS (mean \pm sd of $n = 5$ measurements).

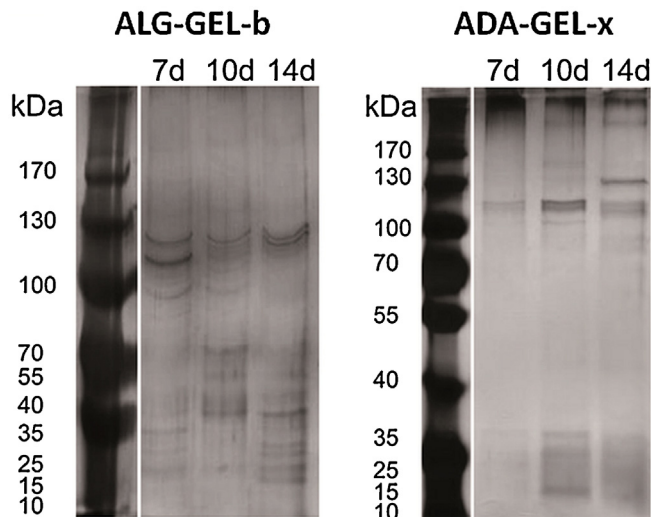


Fig. 3. SDS-page analysis of proteins released from ALG-GEL-b and ADA-GEL-x hydrogels after 7, 10, and 14 days of incubation.

non-crosslinked composition (ALG-GEL-b) during the incubation period (Fig. 2) may have further contributed to a lower storage modulus. Interestingly, ADA-GEL-x hydrogels show the lowest storage modulus and the highest loss tangent at all time points, which we attribute to a diminished network density due to cleavage of vicinal glycols during the oxidation process of alginate [6,25]. Moreover, the mechanical rigidity of gelatin crosslinks may be lower than that of the crosslinks with calcium ions. Despite of the crosslinking, gelatin also diffuses out of the matrix, although with lower amounts compared to alginate-gelatin blends (Fig. 2), as investigated in more detail below.

3.1.2. Gelatin release

Proteins are known to be released from alginate matrices by diffusion through the hydrogel pores or by degradation of the hydrogel network [26]. Our data show that the release kinetics of gelatin was similar for both hydrogels initially, but started to diverge after 7 days of incubation, with a higher gelatin release rate from ALG-GEL-b hydrogels. Moreover, gelatin release from the ADA-GEL-x gels eventually stopped toward the end of the 28 days incubation period but continued in ALG-GEL-b gels. The different behavior in the release kinetics for the two hydrogels can be attributed to the crosslinking between polysaccharides and

proteins in ADA-GEL-x that resists the release of gelatin better than simple blending [2,13]. In ADA-GEL-x, gelatin is covalently bound with polysaccharide (ADA) through the interaction between the ϵ -amino groups of lysine or hydroxylysine of gelatin and the available aldehyde groups of ADA, as described in detail in our previous publication [2].

To analyze the molecular mass of released proteins in the supernatant (HBSS) after 7, 10, and 14 days of incubation, we performed an SDS-PAGE analysis (Fig. 3). In a previous study, we observed that pure gelatin exhibits a wide molecular mass distribution ranging from 53 to 180 kDa [13] with several prominent bands due to the presence of polypeptides of α -chains [13,27,28]. In the present study, we found that after 7 days of incubation, the gelatin released from ALG-GEL-b also showed a number of bands distributed over the range of 70–150 kDa. For longer incubation periods, bands with a molecular mass larger than 100 kDa slowly disappeared, with new bands appearing below 70 kDa. This result indicates that during the incubation period, the gelatin molecules were fragmented to lower molecular mass protein derivatives due to hydrolysis.

The gelatin released from ADA-GEL-x hydrogels after day 7 of incubation showed bands that were distributed over a smaller range around 110 kDa, and new bands that appeared after 10 or 14 days of incubation had for the most part a much lower molecular mass (from 15 to 35 kDa).

3.1.3. Change of microcapsule size

Fig. 4 shows changes in the average diameter of ALG, ALG-GEL-b and ADA-GEL-x microcapsules over an incubation period of 28 days in DMEM. Initially, the diameter of ALG microcapsules increased as the hydrogel swelled, but decreased after 14 days due to the degradation process, as demonstrated elsewhere [2]. Microcapsules fabricated from ALG-GEL-b hydrogel showed a similar trend of swelling and degradation. By contrast, the diameters of ADA-GEL-x microcapsules did not display the initial swelling behavior and steadily decreased from the beginning. As discussed before, ADA is an oxidized derivative of alginate, possessing lower molecular mass compared to alginate due to cleavage of vicinal glycols during partial oxidation of alginate that might have contributed to the higher degradability of ADA-GEL-x [2,13,25]. Moreover, fewer G-units of ADA-GEL-x are available to interact with Ca^{2+} ions due to the oxidation process [2,29], and the anionic groups of G-units may additionally be masked by the crosslinked gelatin molecules, which leads to fast degradation.

We found no obvious difference in diameter of microcapsules over time with and without encapsulated cells, demonstrating that

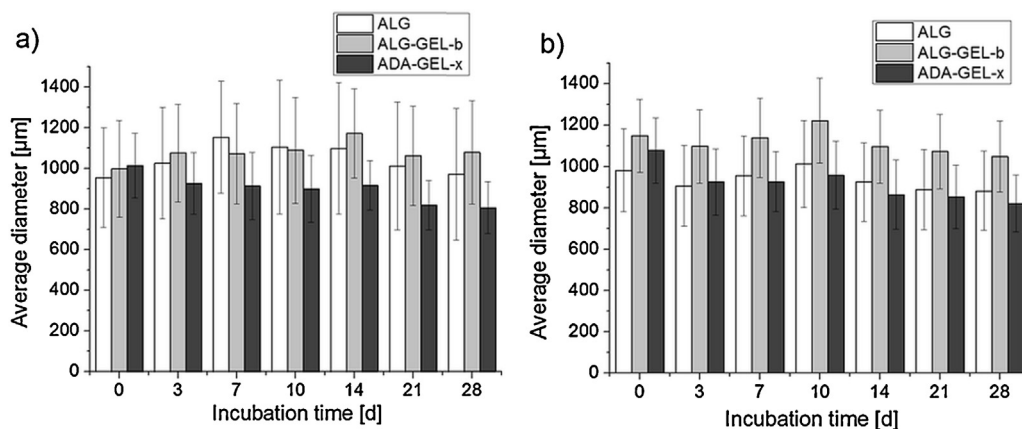


Fig. 4. Average diameter of microcapsules without (a) and with (b) encapsulated cells for ALG, ALG-GEL-b and ADA-GEL-x at different points of incubation from 0 to 28 days in DMEM (mean \pm sd of $n = 30$ measurements).

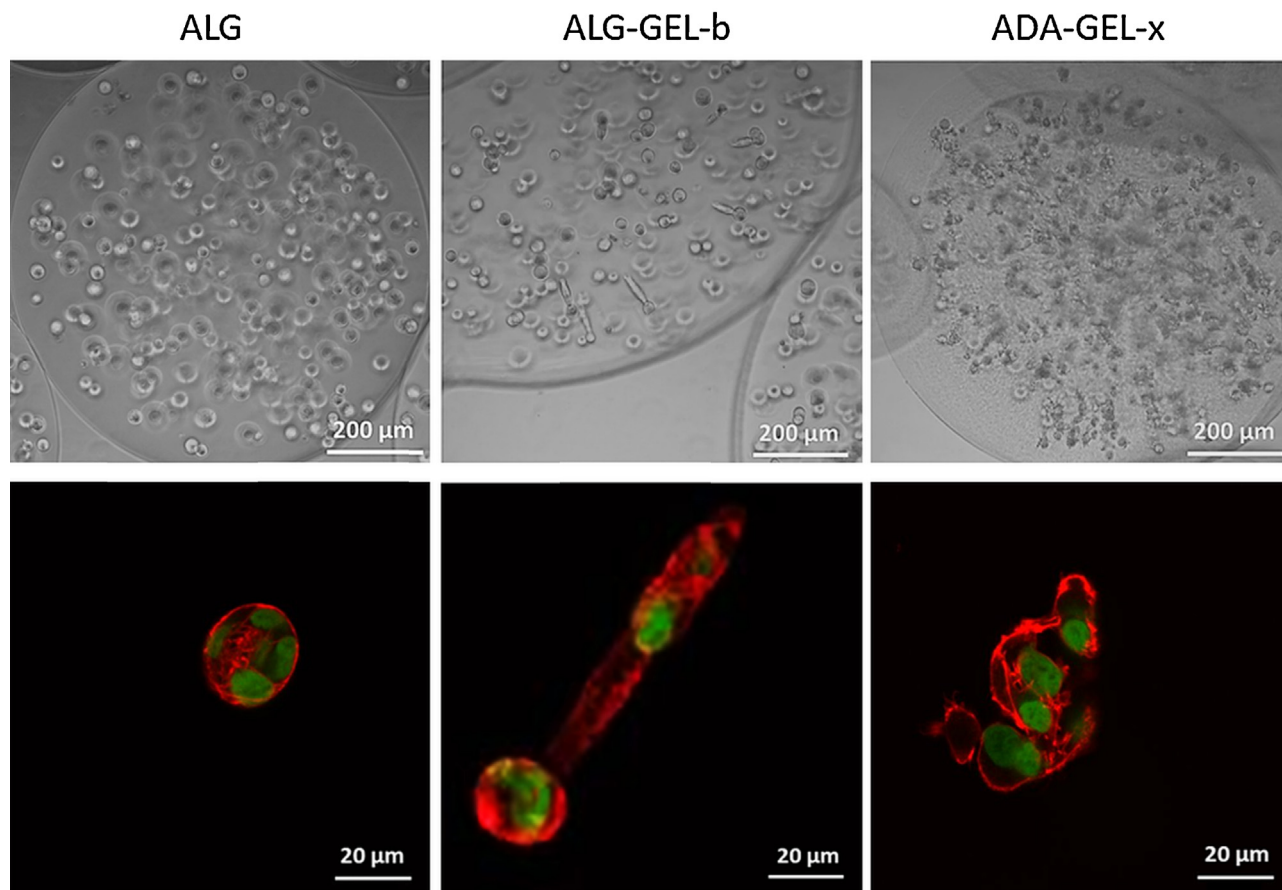


Fig. 5. LM (top row) and CLSM (bottom row) images of cells in ALG, ALG-GEL-b and ADA-GEL-x microcapsules after 7 days of culture. Cells were stained for the nucleus (green) and actin cytoskeleton (red). (For interpretation of references to color in this figure legend the reader is referred to the web version of this article.)

the encapsulated cells had no significant effect on the degradation rate of microcapsules.

3.1.4. Cell morphology

Cell morphology of the encapsulated cells in the different hydrogels was analyzed by bright-field light microscopy (LM) and confocal laser scanning microscopy (CLSM). Fig. 5 shows LM and CLSM images of cells in microcapsules of different materials after 7 days of culture. The cells were found to be uniformly distributed through the whole microcapsules in all three hydrogels. In ALG microcapsules, cells had a round morphology. In ALG microcapsules and in the core of ALG-GEL-b microcapsules, spherical cell clusters formed. In the periphery of ALG-GEL-b microcapsules, however, elongated cell aggregates appeared that were oriented perpendicular to the microcapsule surface. By contrast, cells in ADA-GEL-x microcapsules were usually arranged in irregular shaped clusters, with the individual cells showing a more spread morphology compared to the cells in ALG hydrogels, but not as elongated as some of the cells in the ALG-GEL-b hydrogels.

After 28 days of culture, cells in the ALG and ALG-GEL-b microcapsules were found in spherical clusters, and in the case of ALG-GEL-b hydrogels partially also in elongated cell clusters. Cells in ADA-GEL-x microcapsules, however, were not clustered but instead were seen distributed throughout the entire microcapsules. Moreover, cells were spread, indicating substantial cell–matrix adhesions. Interestingly, some cells had migrated to the surface of ADA-GEL-x microcapsules (Fig. 6) and formed bridge-like structures with cells on the surface of adjacent microcapsule.

The formation of spherical cell clusters in the ALG microcapsules suggests that cell–cell cohesion was stronger than cell–matrix adhesion, in line with the fact that alginate does not possess any cell adhesion molecules. The elongation of the cell clusters seen in the periphery of ALG-GEL-b hydrogel microcapsules, however, is not a sign of strong cell–matrix adhesion. Rather, the gelatin in the blended hydrogels polymerizes into vein-like structures that, upon degradation and gelatin release, leaves behind elongated cavities that are occupied by cells [12]. By contrast, the cross-linked gelatin in the ADA-GEL-x microcapsules facilitated a better cell adhesion. Moreover, in combination with the higher degradation and lower stiffness after several days of culture, better cell spreading and migration were observed in the cross-linked hydrogel in comparison to the other hydrogels investigated.

3.1.5. Cell proliferation and metabolic activity

Cells in the ADA-GEL-x microcapsules showed a higher proliferation than cells in the other two hydrogels. We therefore measured mitochondrial activity as a combined index of the number and metabolic activity of living cells in the microcapsules. After 7 days of incubation, the mitochondrial activity of cells encapsulated in the ADA-GEL-x hydrogels started to significantly ($p < 0.05$) increase (Fig. 7) over the mitochondrial activity of cells encapsulated in the other two hydrogels, reaching a maximum of 150% after 14 days. Interestingly, the mitochondrial activity of cells in the ALG and ALG-GEL-b hydrogels did not increase and even decreased after 14 days despite at least some cell proliferation. This suggests that the metabolic activity in these hydrogels was compromised.

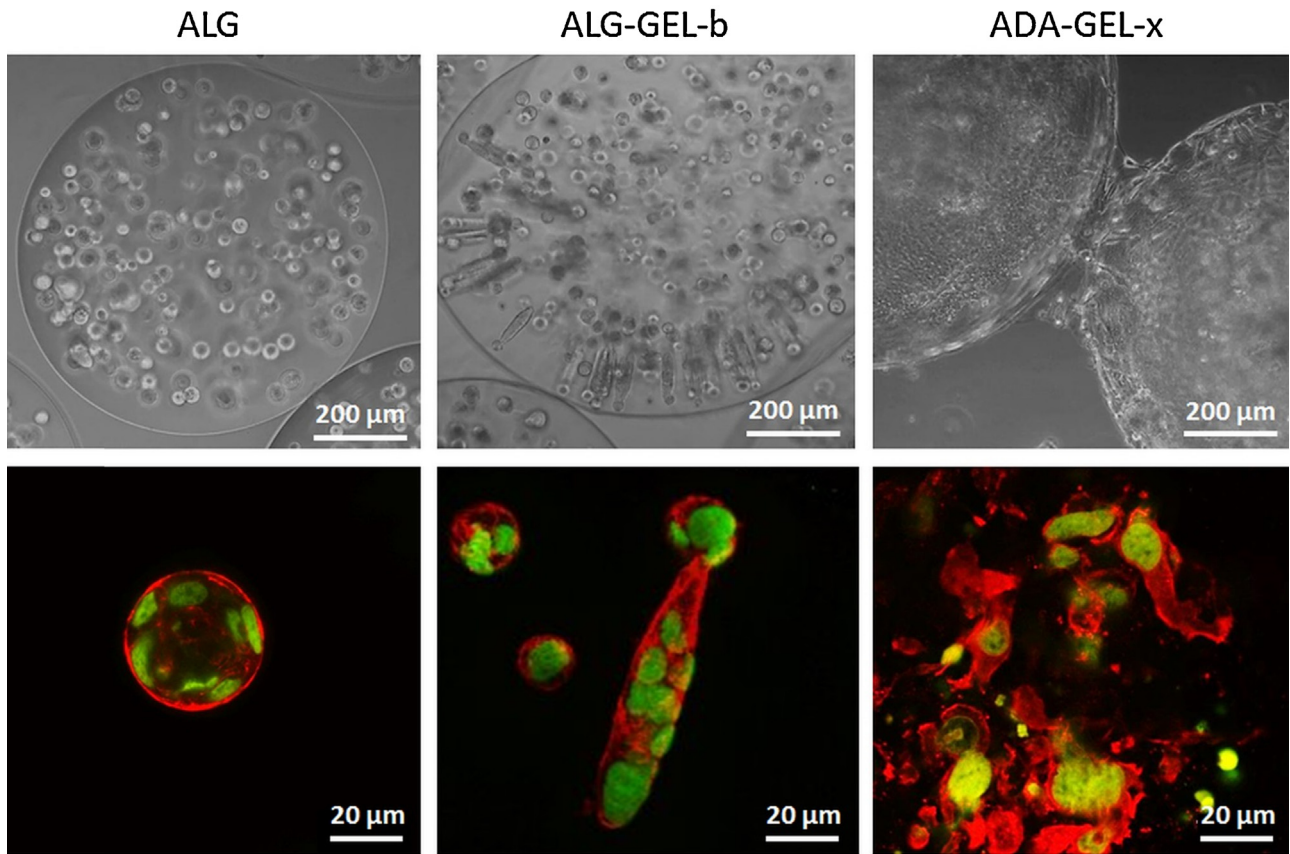


Fig. 6. LM (top row) and CLSM (bottom row) images of cell-loaded ALG, ALG-GEL-b and ADA-GEL-x microcapsules after 28 days of incubation. Cells were stained for the nucleus (green) and actin cytoskeleton (red). (For interpretation of references to color in this figure legend the reader is referred to the web version of this article.)

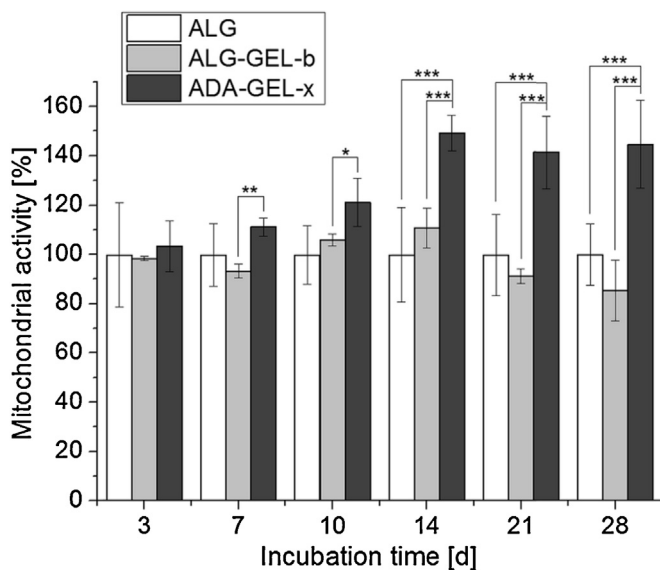


Fig. 7. Mitochondrial activity of encapsulated osteoblast-like cells in ALG, ALG-GEL-b and ADA-GEL-x at different time points of culture. * $p < 0.05$, ** $p < 0.01$ and *** $p < 0.001$.

4. Conclusions

The analysis of three different alginate-based hydrogels revealed similar mechanical properties initially but different degradation rates and cell responses. Pure alginate and gelatin blended alginate did not facilitate cell adhesion and migration, and showed

suppressed metabolic activity after longer incubation times. Cells in the alginate–gelatin crosslinked hydrogels showed good cell adhesion and spreading, and increasing mitochondrial activity after longer incubation times. Alginate–gelatin crosslinked hydrogels exhibited a slower release kinetics of gelatin yet at the same time a faster decrease of stiffness compared to pure alginate or alginate–gelatine blends. We speculate that faster degradation of the hydrogel and the resulting lower stiffness, together with the availability of an adhesive ligand that is tightly bound to the remaining hydrogel matrix, contributed to the better adhesion, spreading, migration, and metabolic activity of the cells in the alginate–gelatin crosslinked hydrogels. These data demonstrate that gelatin crosslinking is a viable strategy to optimize the stiffness and degradation behavior of alginate-based materials for cell encapsulation in tissue-engineering applications.

Acknowledgement

This work was supported by the Emerging Fields Initiative (EFI) of the University of Erlangen–Nuremberg, Germany (project TOPbiomat). Bapi Sarker acknowledges the German Academic Exchange Service (DAAD) for financial support.

References

- [1] A. Murua, A. Portero, G. Orive, R.M. Hernández, M. de Castro, J.L. Pedraz, J. Controlled Rel. 132 (2008) 76–83.
- [2] B. Sarker, D.G. Papageorgiou, R. Silva, T. Zehnder, F. Gul-E-Noor, M. Bertmer, J. Kaschta, K. Chrissafis, R. Detsch, A.R. Boccaccini, J. Mater. Chem. B 2 (2014) 1470–1482.
- [3] J.L. Wilson, T.C. McDevitt, Biotechnol. Bioeng. 110 (2013) 667–682.
- [4] H.-B. Li, H. Jiang, C.-Y. Wang, C.-M. Duan, Y. Ye, X.-P. Su, Q.-X. Kong, J.-F. Wu, X.-M. Guo, Biomed. Mater. 1 (2006) 42–47.

- [5] I.W. Sutherland, *Alignates*, in: *Biomaterials: novel materials from biological sources*, Stockton Press, New York, 1991.
- [6] T. Boonthekul, H.-J. Kong, D.J. Mooney, *Biomaterials* 26 (2005) 2455–2465.
- [7] K.Y. Lee, D.J. Mooney, *Progress Polym. Sci.* 37 (2012) 106–126.
- [8] A.D. Augst, H.J. Kong, D.J. Mooney, *Macromol. Biosci.* 6 (2006) 623–633.
- [9] J.A. Rowley, G. Madlambayan, D.J. Mooney, *Biomaterials* 20 (1999) 45–53.
- [10] W. Zhao, X. Jin, Y. Cong, Y. Liu, *J. Chem. Technol. Biotechnol.* 88 (2013) 327–339.
- [11] K.S. Anseth, C.N. Bowman, L. Brannon-Peppas, *Biomaterials* 17 (1996) 1647–1657.
- [12] A. Grigore, B. Sarker, B. Fabry, A.R. Boccaccini, R. Detsch, *Tissue Eng. Part A* 20 (2014) 2140–2150.
- [13] B. Sarker, R. Singh, R. Silva, J.A. Roether, J. Kaschta, R. Detsch, D.W. Schubert, I. Cicha, A.R. Boccaccini, *PLOS ONE* 9 (2014) e107952.
- [14] E. Boanini, A. Bigi, *J. Colloid Interface Sci.* 362 (2011) 594–599.
- [15] E. Rosellini, C. Cristallini, N. Barbani, G. Vozzi, P. Giusti, *J. Biomed. Mater. Res. Part A* 91 (2009) 447–453.
- [16] S.-C. Wu, W.-H. Chang, G.-C. Dong, K.-Y. Chen, Y.-S. Chen, C.-H. Yao, *J. Bioact. Compatible Polym.* 26 (2011) 565–577.
- [17] O.H. Lowry, N.J. Rosebrough, L. Farr, R.J. Randall, *J. Biol. Chem.* 193 (1951) 265–275.
- [18] G.L. Peterson, *Anal. Biochem.* 83 (1977) 346–356.
- [19] C.M. Güçbilmez, A. Yemeniciolu, A. Arslanolu, *Food Res. Int.* 40 (2007) 80–91.
- [20] N.C. Hunt, A.M. Smith, U. Gbureck, R.M. Shelton, L.M. Grover, *Acta Biomater.* 6 (2010) 3649–3656.
- [21] X. Liu, L. Qian, T. Shu, Z. Tong, *Polymer* 44 (2002) 407–412.
- [22] F. Chambon, *J. Rheol.* 31 (1987) 683–698.
- [23] K. Cai, J. Zhang, L. Deng, L. Yang, Y. Hu, C. Chen, L. Xue, L. Wang, *Adv. Eng. Mater.* 9 (2007) 1082–1088.
- [24] C. Gao, M. Liu, S. Chen, S. Jin, *Int. J. Pharm.* 371 (2009) 16–24.
- [25] K.H. Bouhadir, K.Y. Lee, E. Alsberg, K.L. Damm, K.W. Anderson, D.J. Mooney, *Biotechnol. Progress* 17 (2001) 945–950.
- [26] W.R. Gombotz, S.F. Wee, *Adv. Drug Deliv. Rev.* 64 (2012) 194–205.
- [27] P. Weber, H. Steinhart, A. Paschke, *Food Add. Contam. Part A: Chem. Anal. Control Expos. Risk. Assess.* 27 (2010) 273–282.
- [28] T. Nur Azira, I. Amin, Y.B. Che Man, *Int. Food Res. J.* 19 (2012) 1175–1180.
- [29] C.G. Gomez, M. Rinaudo, M.A. Villar, *Carbohydr. Polym.* 67 (2007) 296–304.
- [30] B. Fabry, G. Maksym, J. Butler, M. Glogauer, D. Navajas, J. Fredberg, *Phys. Rev. Lett.* 87 (2001) 148102.